

Table of Contents

	Page
1. Trotter decomposition error in the quantum simulation of time evolution of the wave function under the S^2 operator	S2
2. Preparation of spin-mixed wave functions on quantum computer	S7
3. Trotter slice number dependence of the probabilistic spin annihilation	S9
4. References	S11

1. Trotter decomposition error in the quantum simulation of time evolution of the wave function under the \mathbf{S}^2 operator

In quantum chemical calculations on quantum computers, the Trotter–Suzuki formula^[1] is frequently used to decompose the time evolution operators onto the sequences of elementary gate operations. Let us consider the time evolution operator $\exp^{i\hbar^{-1}}(-iHt)$ with the Hamiltonian given in eqn (S1).

$$H = \sum_{j=1}^m h_j \quad (\text{S1})$$

The time evolution operator in the first- and the second-order Trotter decomposition is given in eqn (S2) and (S3), respectively.

$$e^{-iHt} \approx \left[e^{-ih_1 t/N} \times e^{-ih_2 t/N} \times \dots \times e^{-ih_m t/N} \right]^N \quad (\text{S2})$$

$$e^{-iHt} \approx \left[\left(e^{-ih_1 t/2N} \times e^{-ih_2 t/2N} \times \dots \times e^{-ih_{m-1} t/2N} \right) \right]^2 \quad (\text{S3})$$

It is known that the Trotter decomposition error depends on the ordering of Hamiltonian terms. The Trotter decomposition error has been well studied in the unitary coupled cluster ansatz for the electronic structure calculations using the variational quantum eigensolver (VQE).^[2–4] A lexicographic ordering can maximize the gate cancellations to reduce the computational costs,^[2] but it is not the best strategy to minimize the Trotter decomposition error. A magnitude ordering gives the smaller Trotter decomposition error than the lexicographic ordering.^[4] More error resilient ordering named as a depleteGroups strategy was also proposed.^[4] However, finding the optimal ordering of Hamiltonian terms to minimize the Trotter decomposition error is generally a difficult task.

In the time evolution of the wave function under the spin operator \mathbf{S}^2 , the magnitude ordering cannot be used because the coefficients of the \mathbf{S}^2 terms are uniform for all molecular orbital indices:

$$\mathbf{S}^2 = \sum_{p,q}^M \left[\frac{1}{4} (a_{p\alpha}^\dagger a_{p\alpha} a_{q\alpha}^\dagger a_{q\alpha} + a_{p\beta}^\dagger a_{p\beta} a_{q\beta}^\dagger a_{q\beta} - a_{p\alpha}^\dagger a_{q\alpha} - a_{p\beta}^\dagger a_{q\beta}) \right] \quad (\text{S4})$$

where M stands for the number of molecular orbitals, $a_{p\sigma}^\dagger$ and $a_{p\sigma}$ for the creation and annihilation operators, respectively, of the p -th molecular orbital of spin- σ ($\sigma \in \{\alpha, \beta\}$). In the present work, we adopted the lexicographic ordering for the quantum simulations of time evolution under the \mathbf{S}^2 operator.

To disclose the Trotter decomposition error, we executed numerical simulations of time evolutions under the \mathbf{S}^2 operator using six electrons in a twelve spin orbital model with randomly prepared initial states with $M_S = 0$. The simulation program was developed by utilising OpenFermion^[5] and Cirq^[6] libraries. The initial states are prepared by the following steps: (1) Initialise the qubit state to $|000\dots 0\rangle$. (2) Apply Pauli-X (NOT) gates to qubits 1–6 to generate a closed shell singlet configuration. Here, the qubits are ordered as $\varphi_{1\alpha}$, $\varphi_{1\beta}$, $\varphi_{2\alpha}$, $\varphi_{2\beta}$, \dots , $\varphi_{6\beta}$. (3) Apply SwapPowGate(i, a) defined in eqn (S5) with random rotation angles

$-1/2 \leq \theta \leq 1/2$, with $i \in$ occupied and $a \in$ unoccupied orbitals, and i and a belong to the same spin symmetry (spin- α or spin- β) to preserve the number of spin- α and spin- β electrons. The obtained wave function is not an eigenfunction of the \mathbf{S}^2 operator, but is an eigenfunction of the \mathbf{S}_z operator. The evolution time T is set to be 10 and changing the number of Trotter slices N in eqn (S2) and (S3) from 40 to 100. Five numerical simulations were executed for each Trotter slice number.

$$\text{SwapPowGate} \doteq \begin{pmatrix} 1 & 0 & 0 & 0 \\ 0 & \cos \frac{\pi}{2}\theta & -i \sin \frac{\pi}{2}\theta & 0 \\ 0 & -i \sin \frac{\pi}{2}\theta & \cos \frac{\pi}{2}\theta & 0 \\ 0 & 0 & 0 & 1 \end{pmatrix} \quad (\text{S5})$$

The square overlap between the wave function obtained from the numerical simulation under the first order Trotter decomposition and the wave function under the exact time evolution without the Trotter decomposition, and the difference of the expectation values of the \mathbf{S}^2 operator calculated with and without the first order Trotter decompositions are depicted in Figures S1 and S2, respectively, and those of the second order Trotter decomposition are summarised in Figures S3 and S4.

Clearly, the first order Trotter decomposition with the Jordan–Wigner transformation (JWT, plots in blue) exhibit very large Trotter decomposition errors. The deviations from the wave function under the exact time evolution become smaller for the larger Trotter slices N , but the error is still not negligible even for $N = 100$. The $\langle \mathbf{S}^2 \rangle$ values of the wave functions under the first order Trotter decomposition oscillate periodically. The fluctuation of the $\langle \mathbf{S}^2 \rangle$ value becomes smaller for the larger N , but the period of the oscillation does not change. We found that the period depends on the number of electrons and the M_S values, as plotted in Figure S5. The mechanism of the oscillations of the $\langle \mathbf{S}^2 \rangle$ value is unclear. We do not discuss this finding further because it is out of the scope of this paper. The Trotter decomposition error can be attenuated by adopting the second order Trotter decomposition, but the fluctuation of the $\langle \mathbf{S}^2 \rangle$ value does not vanish completely for $N = 60$.

In contrast with the JWT, the generalized spin coordinate mapping (GSCM)-based quantum circuit simulations (plotted in red) give the smaller Trotter decomposition error than those of the JWT. The square overlap with the wave function under the exact time evolution is very close to unity for $N \geq 60$, and the $\langle \mathbf{S}^2 \rangle$ value does not oscillate even in the first order Trotter decomposition. From these results we concluded that the GSCM with the second order Trotter decomposition is very reliable and suitable for the quantum simulations of time evolutions under the \mathbf{S}^2 operator from the viewpoint of the Trotter decomposition error.

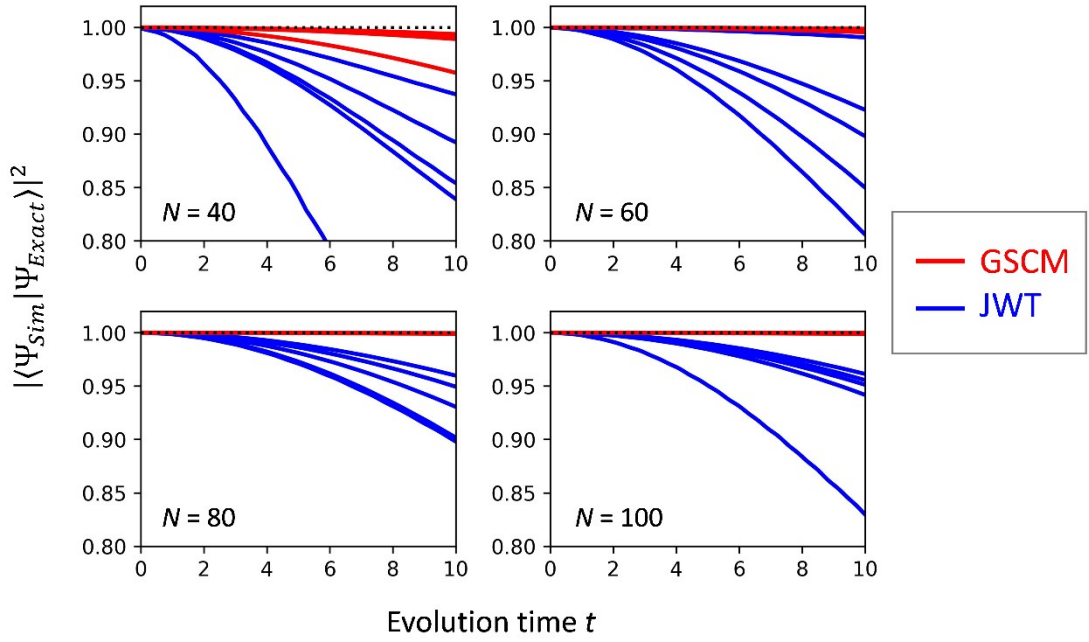


Figure S1. Square overlap of the wave functions with the first order Trotter decomposition with different Trotter slices and that with the exact time evolution. Results using the Jordan–Wigner transformation (JWT) are plotted in blue, and those using generalized spin coordinate mapping (GSCM) are given in red.

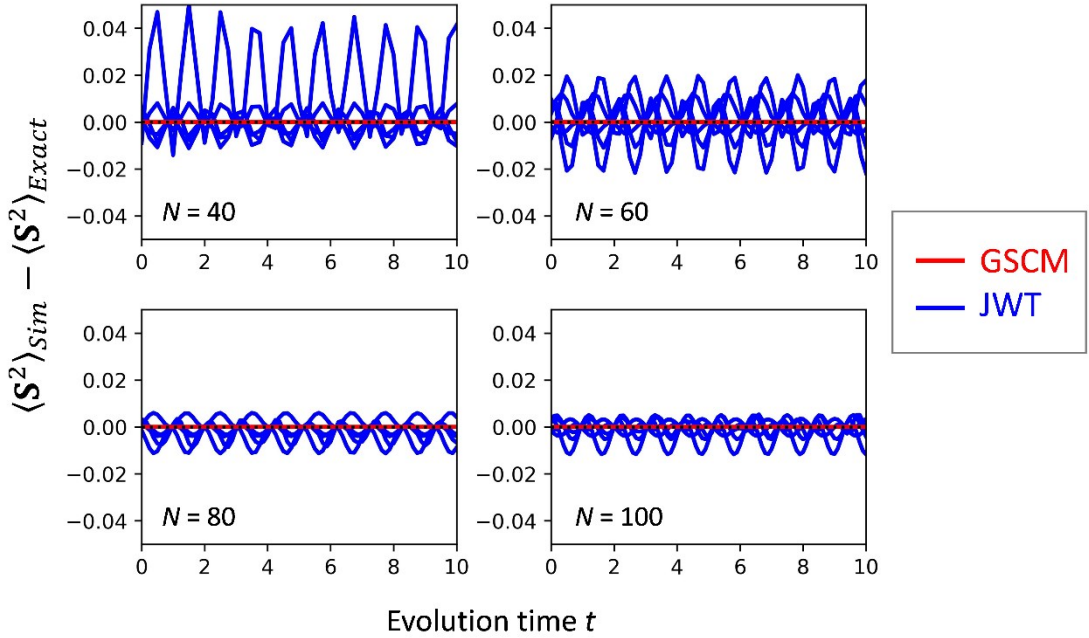


Figure S2. Difference of the expectation values of the S^2 operator calculated with and without the first order Trotter decompositions, with different Trotter slices. Results using Jordan–Wigner transformation (JWT) are plotted in blue, and those using generalized spin coordinate mapping (GSCM) are given in red.

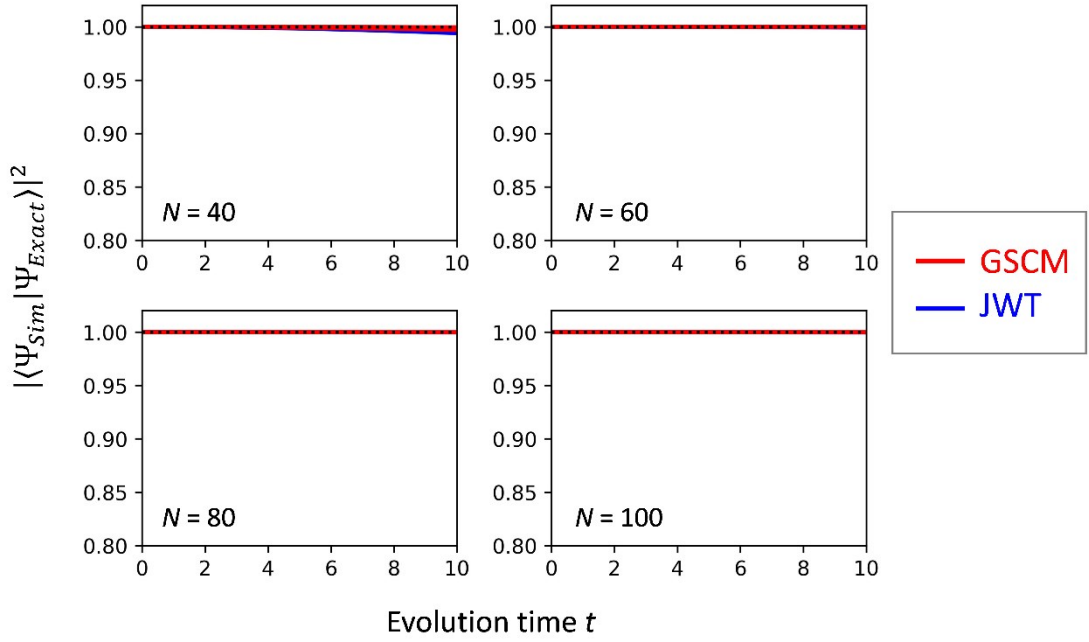


Figure S3. Square overlap of the wave functions with the second order Trotter decomposition with different Trotter slices and that with the exact time evolution. Results using the Jordan–Wigner transformation (JWT) are plotted in blue, and those using generalized spin coordinate mapping (GSCM) are given in red.

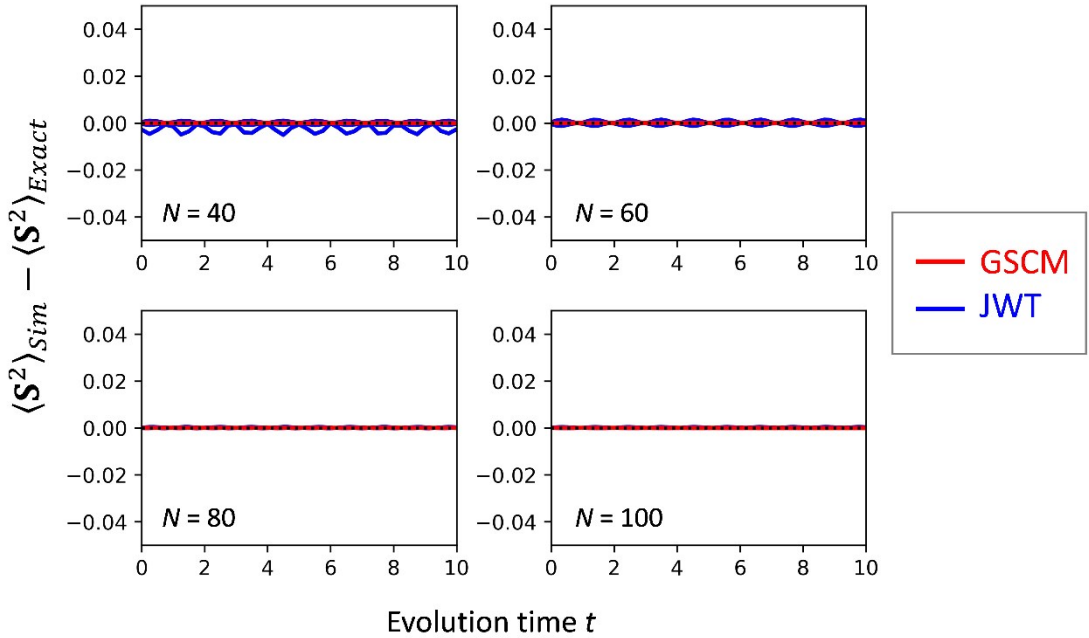


Figure S4. Difference of the expectation values of the S^2 operator calculated with and without the second order Trotter decompositions, with different Trotter slices. Results using the Jordan–Wigner transformation (JWT) are plotted in blue, and those using generalized spin coordinate mapping (GSCM) are given in red.

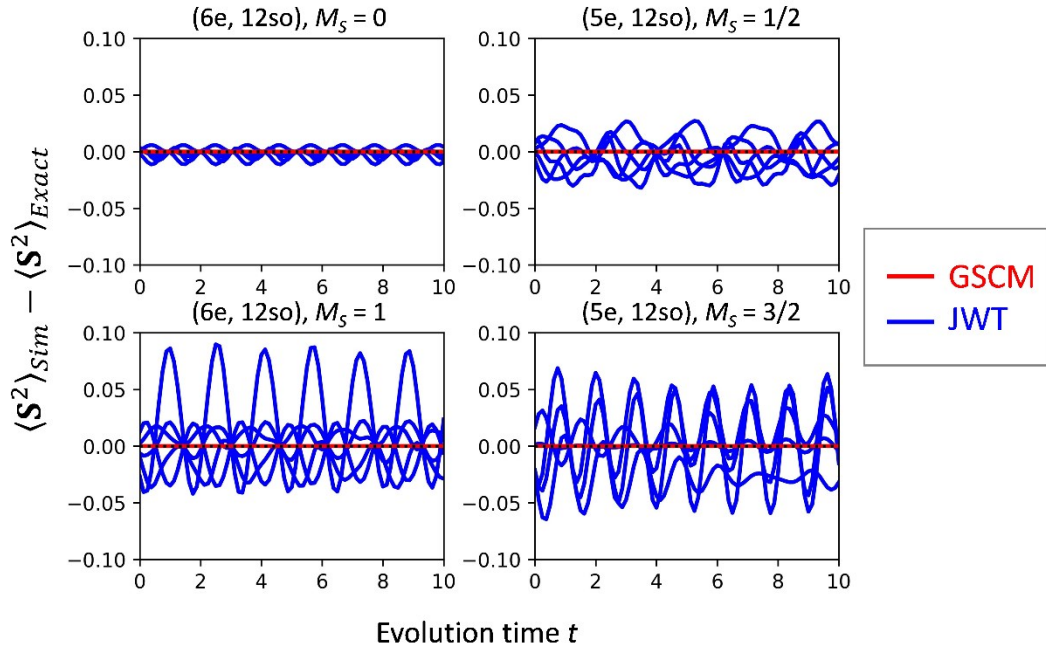


Figure S5. Difference of the expectation values of the \mathbf{S}^2 operator calculated with and without the first order Trotter decomposition with Trotter slices $N = 80$, with the different number of electrons and the M_S values. Results using the Jordan–Wigner transformation (JWT) are plotted in blue, and those using generalized spin coordinate mapping (GSCM) are given in red.

2. Preparation of spin-mixed wave functions on quantum computers.

For the demonstration of the PSA, we generated the spin-mixed wave function which consists of spin-singlet ($|\Psi_{S=0}\rangle$) and spin-triplet ($|\Psi_{S=1}\rangle$) components. Here, $|\Psi_{S=0}\rangle$ and $|\Psi_{S=1}\rangle$ are given in eqn (S6) and (S7), respectively.

$$|\Psi_{S=0}\rangle = \frac{1}{\sqrt{2}}(|2ud0\rangle - |2du0\rangle) \quad (\text{S6})$$

$$|\Psi_{S=1}\rangle = \frac{1}{\sqrt{2}}(|2ud0\rangle + |2du0\rangle) \quad (\text{S7})$$

The spin-mixed wave function can be written as in eqn (S8)

$$\begin{aligned} |\Psi_{Cont}\rangle &= c_{S=0}|\Psi_{S=0}\rangle + c_{S=1}|\Psi_{S=1}\rangle \\ &= c_{ud}|2ud0\rangle + c_{du}|2du0\rangle \end{aligned} \quad (\text{S8})$$

To generate the quantum state corresponding to $|\Psi_{Cont}\rangle$ given in eqn (S8), we constructed a quantum circuit depicted in Fig. 2a. The same Figure is also shown here as Figure S6.

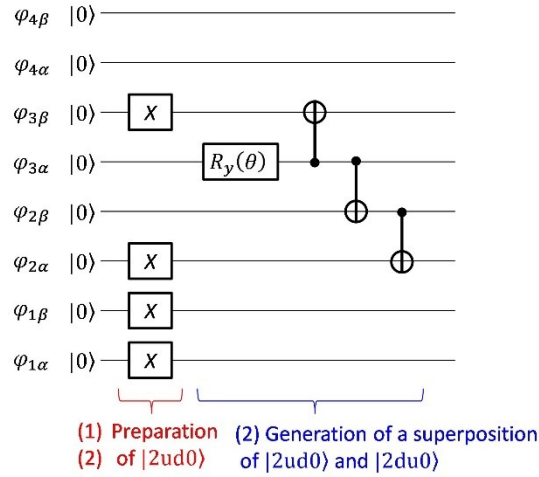


Figure S6. A quantum circuit for the preparation of $|\Psi_{Cont}\rangle = c_{ud}|2ud0\rangle + c_{du}|2du0\rangle$.

The quantum circuit depicted in Figure S6 can be divided into two steps: (1) preparation of the $|2ud0\rangle$ state and (2) generation of a superposition of $|2ud0\rangle$ and $|2du0\rangle$. In the step (1) we applied Pauli-X (NOT) gates on the qubits storing the occupancy of $\varphi_{1\alpha}$, $\varphi_{1\beta}$, $\varphi_{2\alpha}$ and $\varphi_{3\beta}$ orbitals. The resultant quantum state is $|11100100\rangle$, where qubits are ordered as $|\varphi_{1\alpha}\varphi_{1\beta}\varphi_{2\alpha}\cdots\varphi_{4\beta}\rangle$. In the step (2) first we applied a $R_y(\theta)$ gate on the qubit corresponding to $\varphi_{3\alpha}$ orbital. This generate the quantum state in eqn (S9).

$$\cos\frac{\theta}{2}|11100100\rangle - \sin\frac{\theta}{2}|11101100\rangle \quad (\text{S9})$$

Then, we applied three CNOT gates conditioned on the qubit corresponding to $\varphi_{3\alpha}$ orbital. The final quantum state is given in eqn (S10).

$$\cos\frac{\theta}{2}|11100100\rangle - \sin\frac{\theta}{2}|11011000\rangle \quad (\text{S10})$$

The quantum state in eqn (10) corresponds to the spin-contaminated wave function given in eqn (S11).

$$|\Psi_{cont}\rangle = \cos\frac{\theta}{2}|2ud0\rangle - \sin\frac{\theta}{2}|2du0\rangle \quad (\text{S11})$$

By comparing eqn (S8) and (S11) we can derive the following relationship.

$$c_{ud} = \cos\frac{\theta}{2}, c_{du} = \sin\frac{\theta}{2} \quad (\text{S12})$$

If we set $\theta = -\pi/2$ we obtain $c_{ud} = 1/\sqrt{2}$ and $c_{du} = -1/\sqrt{2}$, which corresponds to the spin-singlet wave function in eqn (S6), and in case of $\theta = \pi/2$ we obtain $c_{ud} = c_{du} = 1/\sqrt{2}$, which is the spin-triplet wave function in eqn (S7). By changing θ from $-\pi/2$ to $\pi/2$, we can obtain the spin-mixed wave functions.

3. Trotter slice number dependence of the probabilistic spin annihilation

Because the probabilistic spin annihilations (PSA) proposed in this work use the time evolution of the wave function under the S^2 operator, Trotter decomposition error can affect the spin annihilation results. As discussed in the previous section, the GSCM-based wave function encoding in conjunction with the second order Trotter decomposition gives very small Trotter decomposition error for $T = 10$ and $N \geq 40$, where T denotes the evolution time and N the number of Trotter slices.

In the PSA, for spin-singlet ($S = 0$) and spin-doublet ($S = 1/2$) states the evolution time T is $\pi/2$ and $\pi/3$, respectively. In the main text, we described the PSA results with the second order Trotter decomposition with $N = 2$. This corresponds to $N = 12.7$ and 19.1 for $S = 0$ and $1/2$, respectively, for $T = 10$ described in the previous section. We checked the Trotter slice number dependence on the quality of spin annihilated wave functions obtained from the PSA.

The $\langle S^2 \rangle$ value of the spin annihilated wave function $|\Psi_{Anni}\rangle$ with different Trotter slice numbers for $|\Psi_{Cont}\rangle = |\text{udud}\rangle$ and $|\text{ududu}\rangle$ are summarised in Figure S7 and S8, respectively. The $\langle S^2 \rangle$ value becomes closer to the theoretical value specified by the dotted horizontal line as the number of the Trotter slice increases. The spin annihilated wave functions $|\Psi_{Anni}\rangle$ for $|\Psi_{Cont}\rangle = |\text{udud}\rangle$ and $|\text{ududu}\rangle$ with $N = 5$ are given in eqn (S13) and (S14), respectively.

$$\begin{aligned} |\Psi_{Anni, N=5}^{\text{udud}}\rangle &= (0.5774 + 0.0055i)|\text{udud}\rangle + (0.5773 - 0.0055i)|\text{duud}\rangle \\ &\quad + (-0.2887 + 0.0055i)|\text{dduu}\rangle + (-0.2887 - 0.0055i)|\text{dudd}\rangle \end{aligned} \quad (\text{S13})$$

$$\begin{aligned} |\Psi_{Anni, N=5}^{\text{ududu}}\rangle &= (0.7246 - 0.0578i)|\text{ududu}\rangle + (0.2645 - 0.0578i)|\text{duudu}\rangle \\ &\quad + (0.2645 - 0.0611i)|\text{duduu}\rangle + (-0.1955 - 0.0594i)|\text{uuddu}\rangle \\ &\quad + (-0.1955 - 0.0594i)|\text{udduu}\rangle + (-0.1955 - 0.0594i)|\text{duudu}\rangle + (-0.1955 - 0.0594i)|\text{duddu}\rangle \end{aligned} \quad (\text{S14})$$

The spin annihilated wave function $|\Psi_{Anni}\rangle$ for $|\Psi_{Cont}\rangle = |\text{udud}\rangle$ with Trotter slice $N = 2$ is given in eqn (S15).

$$\begin{aligned} |\Psi_{Anni, N=2}^{\text{udud}}\rangle &= (0.5778 + 0.0324i)|\text{udud}\rangle + (0.5751 - 0.0324i)|\text{duud}\rangle \\ &\quad + (-0.2888 + 0.0322i)|\text{dduu}\rangle + (-0.2882 - 0.0322i)|\text{dudd}\rangle \end{aligned} \quad (\text{S15})$$

By comparing eqn (S13) and (S15), the increase of Trotter slice results in the reduction of the imaginary part of coefficients, and $|\Psi_{Anni}\rangle$ with $N = 5$ is closer to the spin eigenfunction for $S = 0$ given in eqn (17) in the main text.

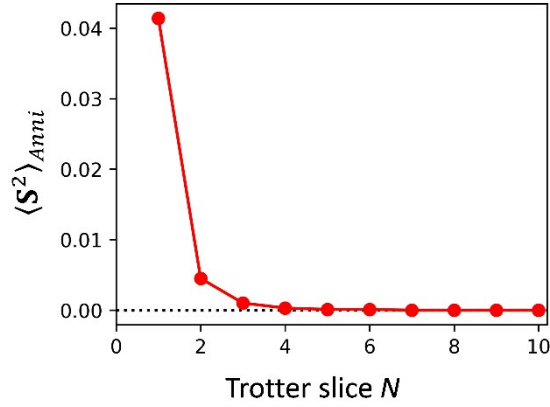


Figure S7. Trotter slice number dependence on the $\langle S^2 \rangle$ value of the spin annihilated wave function starting from $|\Psi_{Cont}\rangle = |\text{udud}\rangle$. The dotted line specifies the theoretical value in the absence of the Trotter decomposition error.

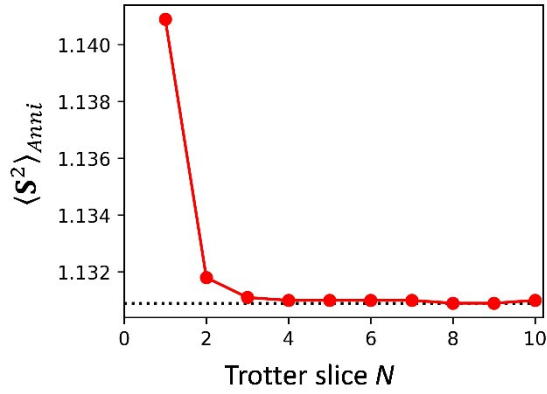


Figure S8. Trotter slice number dependence on the $\langle S^2 \rangle$ value of the spin annihilated wave function starting from $|\Psi_{Cont}\rangle = |\text{ududu}\rangle$. The dotted line specifies the theoretical value in the absence of the Trotter decomposition error.

4. References

- [1] H. F. Trotter, *Proc. Amer. Math. Soc.*, 1959, **10**, 545–551.
- [2] A. Tranter, P. J. Love, F. Mintert and P. V. Coveney, *J. Chem. Theory Comput.*, 2018, **14**, 5617–5630.
- [3] H. R. Grimsley, D. Claudino, S. E. Economou, E. Barnes and N. J. Mayhall, *J. Chem. Theory Comput.*, 2020, **16**, 1–6.
- [4] A. Tranter, P. J. Love, F. Mintert, N. Wiebe and P. V. Coveney, *Entropy*, 2019, **21**, 1218.
- [5] J. R. McClean, N. C. Rubin, K. J. Sung, I. D. Kivlichan, X. Bonet-Monroig, Y. Cao, C. Dai, E. S. Fried, C. Gidney, B. Gimby, P. Gokhale, T. Häner, T. Hardikar, V. Havlíček, O. Higgott, C. Huang, J. Izaac, Z. Jiang, X. Liu, S. McArdle, M. Neeley, T. O’Brien, B. O’Gorman, I. Ozfidan, M. D. Radin, J. Romero, N. P. D. Sawaya, B. Senjean, K. Setia, S. Sim, D. S. Steiger, M. Steudtner, Q. Sun, W. Sun, D. Wang, F. Zhang and R. Babbush, *Quantum Sci. Technol.*, 2020, **5**, 034014.
- [6] Cirq. <https://github.com/quantumlib/Cirq>